Kinematics of the Asal Rift (Djibouti) Determined from the Deformation of Fieale Volcano

Jean-Bernard De Chabalier* and Jean-Philippe Avouac

Because of its subaerial exposure the Asal rift segment provides an exceptional opportunity to quantify the deformation field of an active rift and assess the contribution of tectonics and volcanism to rifting processes. The present topography of the Asal rift results from the tectonic dismemberment during the last 100,000 years of a large central volcanic edifice that formed astride the rift zone 300,000 to 100,000 years ago. Three-dimensional deformation of this volcano has been quantified from the combined analysis of the topography and geology. The analysis indicates that spreading at 17 to 29 millimeters per year in a N40° ± 5°E direction accounts for most of the separation between Arabia and Somalia. The small topographic subsidence relative to extension suggests that tectonic thinning of the crust has been balanced by injection and underplating of magmatic material of near crustal density. The methodology developed in this study could also be applied to quantify deformation in relatively inaccessible areas where the main available information is topography or bathymetry.

The Afar Depression at the triple junction between Arabia, Somalia, and the rest of Africa (Fig. 1), is characterized by active continental stretching and volcanism (*1*). Although the large-scale kinematics of this triple junction is well constrained from global plate tectonics (*2–4*), the detailed deformation of the Afar Depression is still a matter of debate (*5, 6*). In this paper we focus on the Asal rift at the western end of the Gulf of Aden rift (Fig. 1), which is propagating westward at about 30 mm/year into the Afar Depression (*7*). The Asal rift has long been recognized as an emerged analogue to slow spreading ridges (*1*) where active tectonics and volcanism can be observed directly (*8*). Because of the lack of oceanic magnetic anomalies (*7*) and of clearly defined transform faults (*5*), the long-term direction and rate of spreading across the rift have been poorly constrained. We show that this information can be determined from the combination of high-resolution topography (digital elevation model, DEM) and geological and geochronological data. We have reconstructed the initial three-dimensional geometry of a major volcanic edifice, the Fieale volcano, that formed astride the rift and was deformed by rifting over the last ~100,000 years. This reconstruction moreover allows assessment of the relative contribution of magmatism and tectonics during rifting. This approach could also be applied to high-resolution bathymetric data to derive the direction of spreading along oceanic ridges, independently of fracture zones or magnetic anomalies.

The Modern Asal Rift Zone

The 15-km-long subaerial exposure of the Asal rift connects Lake Asal with Ghoubbet Bay, which is the continuation of the Gulf of Aden–Tadjoura ridge (Fig. 1). Only minor erosion and deposition seems to have occurred since the formation of the basaltic rift floor; thus, the topography of the rift provides a well-preserved record of tectonic deformation (*9, 10*). Steep normal fault scarps with throws of up to 150 m can be easily distinguished on the DEM (Fig. 2). They roughly parallel the trend of the rift (mean fault strike is N127°E with a 20° standard deviation) and are concentrated in a narrow band about 10 km wide. Slopes between fault scarps generally dip gently away from the rift axis and are thought to reflect the surface of tilted fault blocks (*11*). Most of the faults are slightly curved toward the rift axis, particularly those close to Fieale crater (Fig. 2). In all, the axial valley is narrower and shallower in the middle than at the ends of the segment, a typical hourglass shape, as has been observed along oceanic ridges (*12, 13*).

The modern Asal rift formed after the flooding of the Stratoid Series basalts on the floor of the Afar Depression between 4 million and 1 million years ago (*14*). Three subsequent basalt series characterize the rift magmatism. The Initial Series basalts mark the initiation of rifting in the Gulf of Tadjoura (*15, 16*) and end with a hyaloclasite

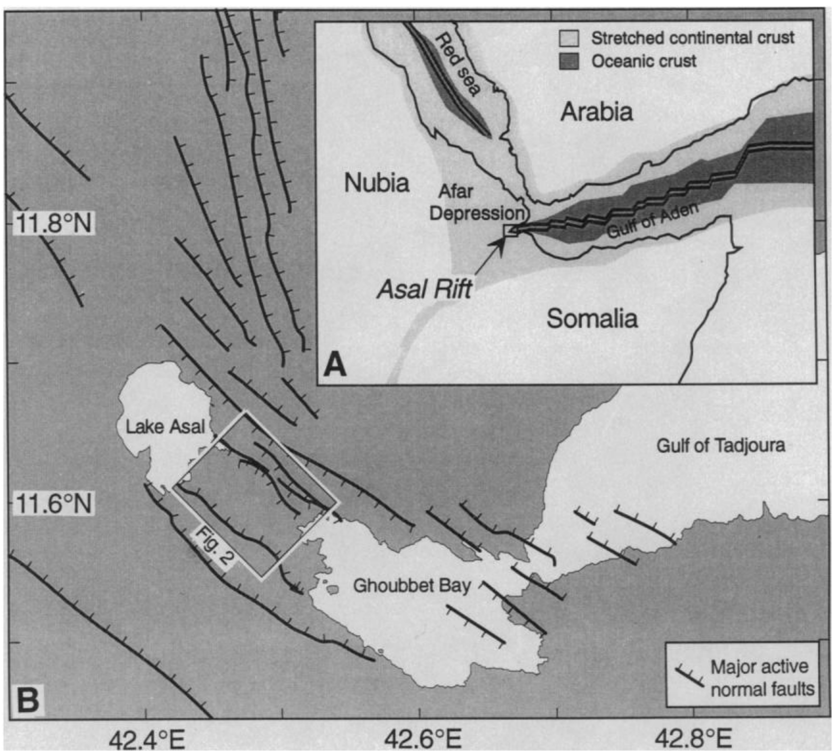

Fig. 1. (**A**) Map of Afar Triple Junction. The box shows location of (B). (**B**) Tectonic map of the Asal-Ghoubbet region [from (*5*)]. The box shows location of Fig. 2.

J.-B. De Chabalier is in the Équipe de Sismotectonique, Institut de Physique du Globe, 4 Place Jussieu, 75252 Paris Cedex 05, France. J.-P. Avouac is in the Laboratoire De Géophysique, Commissariat à l'Énergie Atomique (CEA), B.P. 12, Bruyères-le-Chatel 91680, France.

*Present address: Laboratoire De Géophysique, CEA, B.P. 12, Bruyères-le-Chatel 91680, France.

eruption episode at about 300,000 years ago (300 ka) (Fig. 3) (*17*). The Central Series consist of younger basalts of oceanic affinity (*18*). They are spread over the inner floor (Fig. 3) and are more than 300 m thick near the rift axis (well A5, Fig. 3) (*19*). These lavas were erupted from the Fieale volcano, as indicated by the divergence of the flow lines (Fig. 3). Most of the flow appears to have been perpendicular to the present elevation contour lines (Fig. 2), indicating that little tilting has occurred since the basalt was deposited. This magmatic episode lasted from about 300 to 65 ka (*17*). Whereas basaltic flows older than 150 ka have apparently spread astride the rift zone, flows younger than 87 ka abut fault scarps and therefore tend to have concentrated near the rift axis (Fig. 3) (*20*). Later, the magmatic activity within the Asal rift resumed significantly. Small volcanic edifices aligned along an eruptive fissure in the inner floor fed a minor volcanic episode (Axial Series, Fig. 3) that postdates early Holocene lacustrine sediments (*21*). The thickness of the Axial Series around Fieale crater is ~20 m (well A5, Fig. 3). Overall, therefore, the topography and the geology of the rift zone is that of a major volcanic edifice fed by the Fieale crater, which has recorded tectonic deformation over the last 87,000 to 150,000 years.

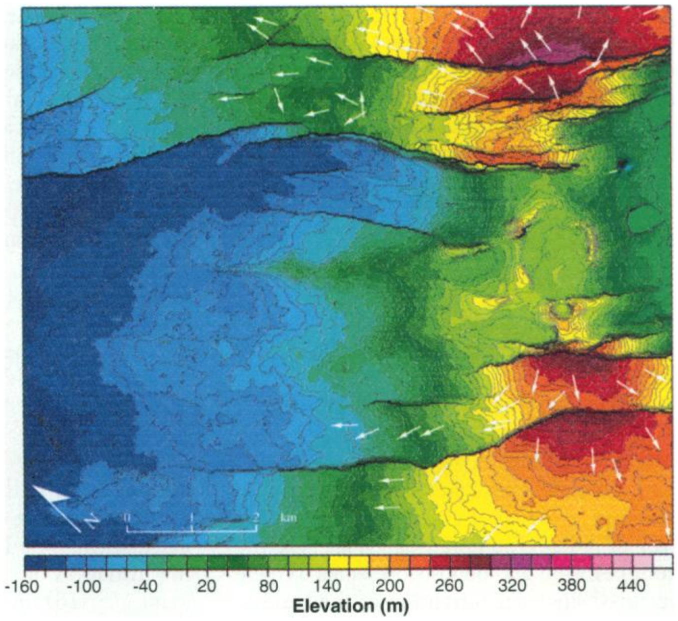

Fig. 2. High resolution Digital Elevation Model of the Asal rift. [Courtesy of French Institut Géographique National] Uncertainties on elevation are about 1 to 2 m. Arrows indicate basalt flows [from (*16*)].

Restoration of Vertical Displacements

We determined vertical offsets on the faults on a series of cross sections spaced every 15 m oriented perpendicular to the rift axis. To take into account erosion at crest and deposition at base of the scarps, the topography was linearly extrapolated onto the fault plane. For a nonvertical fault and a nonhorizontal topography the measured vertical offset of the topographic surface differs systematically from the vertical throw on the fault by

$$dz = \tan\beta/(\tan\Phi + \tan\beta) \qquad (1)$$

where β is the regional slope and Φ is the fault dip. Field investigation (*11*, *19*, *22*), as well as modeling of the ground deformation associated with the 1978 seismovolcanic event (*10*), have shown that the faults are steep with dip angles in excess of 80° near the surface, and because regional slopes do not exceed 10°, calculated vertical throws

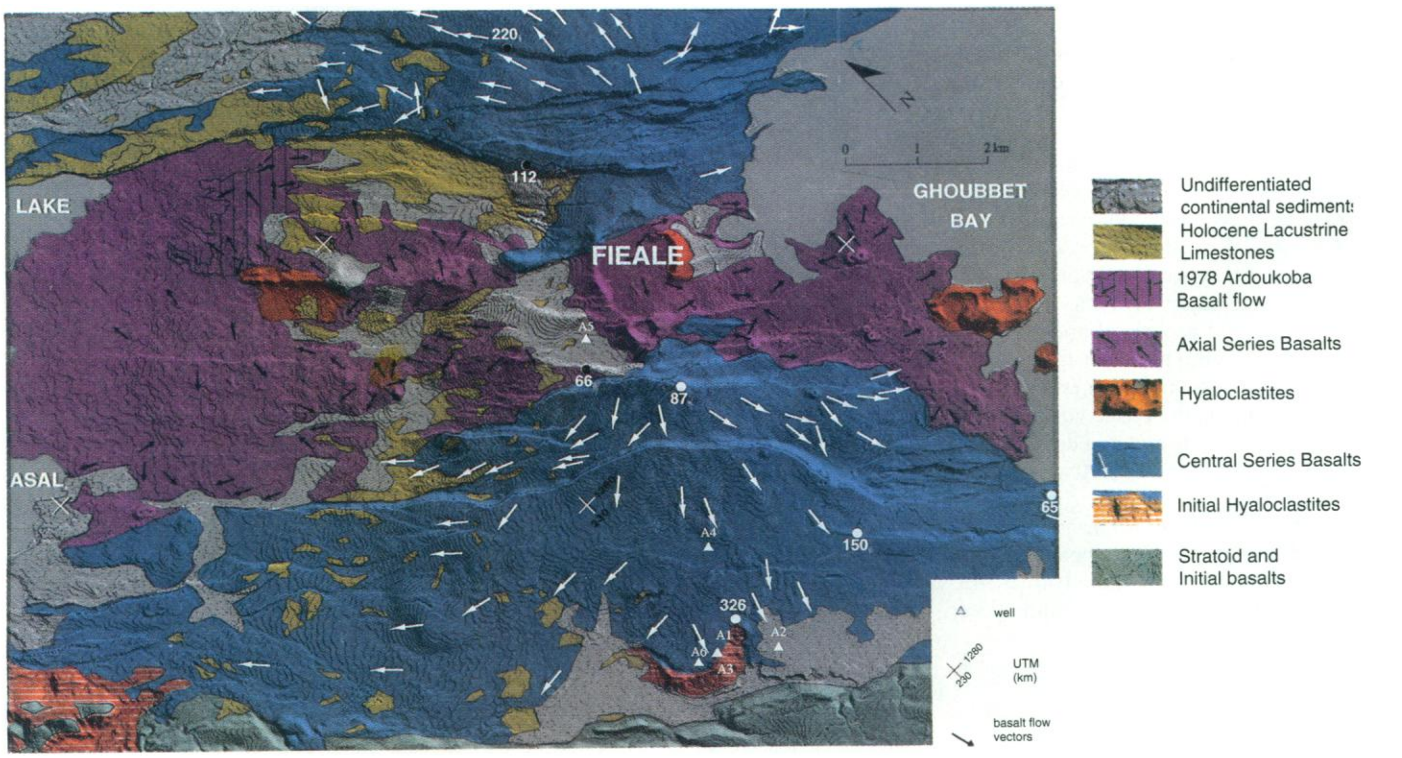

Fig. 3. Geological map of the Asal rift [simplified from (*16*, *19*)] superimposed on shaded topography (DEM). Arrows indicate direction of basalt flows. Circles are location of K-Ar dats in thousand years (*17*), sampled at the surface (white) or into fault scarp outcrops (black).

might be in error by 3% at most. Vertical throws on the major faults are typically ~100 m, and the cumulative vertical throw across the rift zone is ~700 m, corresponding to about 350 m of subsidence at the rift axis relative to the rift flanks, 5 km away from rift axis.

We restored the topography across the rift to a continuous surface by subtracting the vertical offsets on the faults. This restoration was made along serial topographic profiles with arbitrarily chosen azimuths, that ran across the rift (Fig. 4). If the restored topography is held fixed with respect to the southwest rift shoulder, the restored northeast shoulder appears vertically offset down by an amount *dh* (Fig. 4). If instead the northeast shoulder is fixed, the southwest shoulder is lifted by *dh*. We chose a reference frame in which *dh* is equally distributed to the southwest and northeast of the rift (Fig. 4). We then searched different profiles with azimuths between 15° and 50° to find a model with as little deformation (*dh*) as possible outside the rift zone. The minimum standard deviation of *dh* (17 m) occurred for N30°E profiles. This solution indicates that the mean downthrow of the southwest shoulder with respect to the northeast shoulder (*dh*) is 30 m and suggests that extension was slightly oblique.

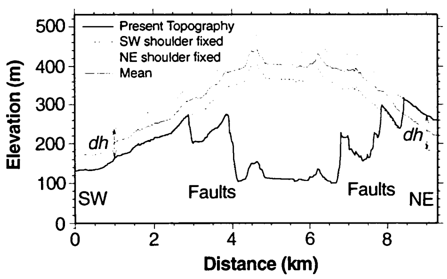

Fig. 4. Vertical reconstruction of a profile across the rift. Thick line is present topography. Dashed line is restored profile for SW rift shoulder held fixed, creating NE shoulder offset (*dh*). If instead the NE shoulder is fixed (dotted line), the SW shoulder is also offset by *dh*. Thin continuous line is the mean between these two restored profiles, distributing equally the offset in the SW and the NE shoulder.

Restoration of Horizontal Displacements

A striking feature of the vertically restored topography of the Fieale volcanic edifice is the ellipticity of the elevation contour lines (Fig. 5A). Undeformed volcanoes are commonly axisymmetric. Although a volcano can be elongated if fed by several aligned eruptive centers or fissures, the elongation visible in Fig. 5A is probably of tectonic origin because it is perpendicular to the trend of the eruptive centers and fissures. Thus, the departure from an assumed initial axisymmetry of the Fieale volcano can be used to determine the direction and amount of extension across the Asal rift. Vertical displacements due to normal faulting are nearly linearly distributed across the rift zone. We therefore assumed that the horizontal deformation within the rift was homogeneous. We further assumed that the volcano has suffered no elongation in the direction of the mean fault strike (θ_0 = N127°E ± 20°). If the direction of no elongation (θ_0) is taken to be $0x$ (Fig. 6), the horizontal displacement field, considering no translational motion, is

$$x = x' + s\lambda y' \qquad (2)$$

$$y = \lambda y' \qquad (3)$$

where (x, y) refer to the present coordinates of a point that had (x', y') coordinates before deformation; λ is the elongation, and s is the fault parallel shear. The reference frame might have rotated, but such a rotation cannot be resolved from the deformation of the Fieale volcano. For this displacement field, the total extension experienced by a domain of final width W is

$$E = W(1 - 1/\lambda) \qquad (4)$$

and the total lateral shear is

$$S = sW \qquad (5)$$

If W spans the whole rift zone, we get the total extension and shear across the Asal rift. If $0x$ did not rotate during deformation, the azimuth of the direction of spreading across the rift zone, θ (Fig. 6) is

$$\tan(\theta - \theta_0) = E/S = (1 - \lambda)/s\lambda \qquad (6)$$

We propose that s and λ can be derived from the second-order moments of the vertically restored topography defined by

$$M_{xx} = \iint y^2(z - z_0)dxdy \qquad (7)$$

$$M_{yy} = \iint x^2(z - z_0)dxdy \qquad (8)$$

$$M_{xy} = \iint xy(z - z_0)dxdy \qquad (9)$$

We consider domains of integration defined by $z > z_0$. By varying z_0, we can restrict the computation to the summit of the volcano or consider a zone spanning the whole rift (z_0 > 300 m, Fig. 5A).

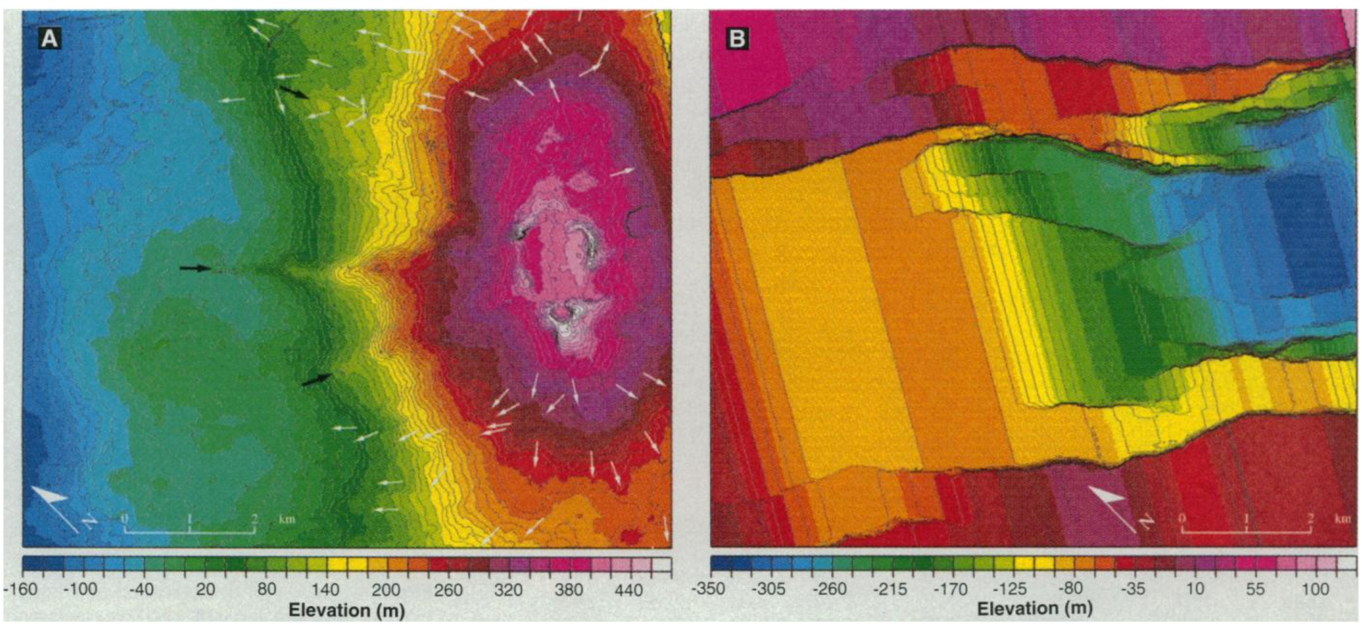

Fig. 5. Resulting topography (**A**) after restoration of vertical throws on faults according to vertical displacements model of (**B**). Direction of flows from Fig. 3. Black arrows point to some dikes that show off in the topography.

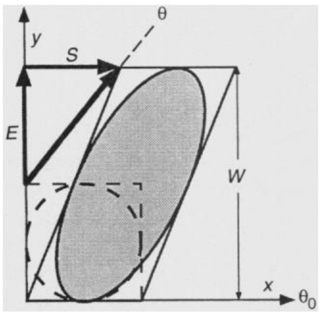

Fig. 6. Deformation field assuming no elongation along 0*x* (with azimuth θ_0) and no rotation of 0*x*. A circular marker is deformed into an ellipse. θ is the direction of spreading. *E* and *S* are respectively the finite extension and lateral shear experienced by a domain of width *W*.

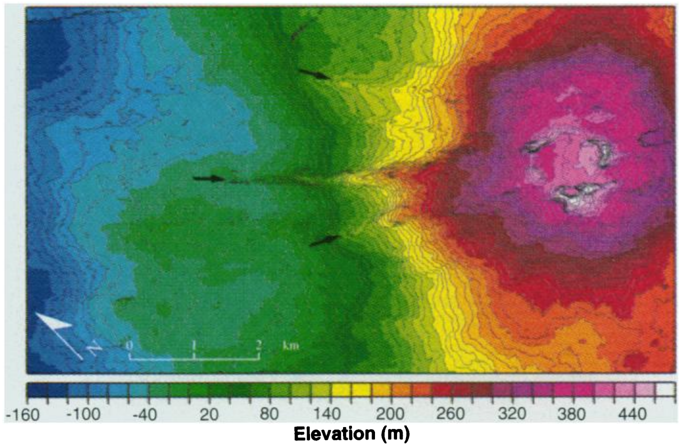

Fig. 7. Topography of the Fieale volcano after restoration of distributed extension (2550 m) perpendicular to mean faults strike and distributed shear (109 m) parallel to rift axis.

The topography of the initial axisymmetric volcano must satisfy

$$M'_{yy} = M'_{xx} \quad (10)$$

$$M'_{xy} = M'_{yx} = 0 \quad (11)$$

According to the displacement field (Eqs. 2 and 3), we must also have

$$M_{xx} = \lambda^3 M'_{yy} \quad (12)$$

$$M_{yy} = \lambda M'_{xx} + \lambda^3 s^2 M'_{yy} \quad (13)$$

$$M_{xy} = M_{yx} = s\lambda^3 M'_{xx} \quad (14)$$

We then infer

$$\lambda = [M_{xx}^2/(M_{xx}M_{yy} - M_{xy}^2)]^{1/2} \quad (15)$$

$$s = M_{xy}/M_{xx} \quad (16)$$

Values of the moments and λ, *E*, *s*, *S*, and θ are given in Table 1 for different values of z_0 and for $\theta_0 = 127°$. For this reference frame, the three-dimensional reconstruction of the Fieale volcano (Fig. 7) reveals that there has been 2550 m of elongation and 109 m of right lateral shear across the whole rift (Table 1). The calculated elongation and the horizontal shear tend to be greater for higher values of z_0. This trend would indicate that the deformation was slightly heterogeneous such that stretching and shear were more intense close to the rift axis. This result suggests that the zone of active stretching has remained fixed during deformation with a width of ~4 km. Given that the direction of no elongation (θ_0) is not very well constrained, we made computations for different values between plausible extremes (N120°E and N135°E). The total extension is not very sensitive to this parameter (Fig. 8), and the cumulative shear remains small in comparison to the total extension and varies between 500 m of right-lateral shear and 600 m of left-lateral shear. The preferred value for θ_0 (N127°E) is near that corresponding to pure rifting (N128.5°E). The spreading direction is relatively well constrained between N35°E and N43°E (Fig. 8).

Implications

The 2.6 km of extension recorded by Fieale volcano since about 150 to 87 ka yields a spreading rate of 17 to 29 mm/year. This rate and the spreading azimuth (N40 ± 5°), obtained assuming no rotation of the faults during deformation, compare well with the Arabia-Somalia plate kinematic vector (*3*, *4*) computed at a point within the Asal rift (Fig. 9). This comparison would suggest that most of the present motion between Arabia and Somalia is accommodated by the Asal rift. We conclude that, at the location of the Asal rift, the transition from continental to oceanic rifting is probably complete.

Although the present topography of the rift is generally interpreted to reflect normal fault blocks tilted away from the rift axis, our modeling shows, in agreement with paleomagnetic evidence (*23*) and basalt flow vectors (*16*), that such tilts are not required; the slopes have most probably been inherited from the initial shape of the volcano.

The deformation model of Fig. 5B indicates that the subsidence of the inner floor of the Asal rift has not been uniform. Vertical displacements are much larger near the crater of the Fieale volcano where the axial valley is narrower. Such a pattern could reflect collapse of a magmatic chamber. However, the fault pattern at the surface does not resemble that usually associated with calderas (*24*). Near the Fieale the normal faults are curved toward the crater where they tend to concentrate. This hourglass geometry might reflect the effect on the extensional regional stress field of topographic loading by the central volcanic edifice.

The three-dimensional model of deformation of the Fieale volcano moreover al-

Table 1. Moments (M_{xx}, M_{yy}, $M_{xy} = M_{yx}$) of the Fieale volcano topography after restoration of vertical throws on faults. 0_x is parallel to mean faults strike (N127°E). First column lists base of truncated topography (z_0) delimiting a domain of width *W* used for computation of moments. Next columns list elongation perpendicular to rift axis (λ) and horizontal shear (*s*). Last columns list total extension *E*, total shear *S*, and resulting azimuth of direction of spreading θ across a domain of width *W* (Eqs. 4 to 6).

z_0 (m)	*W* (m)	M_{xx} (10^{13} m^5)	M_{yy} (10^{13} m^5)	M_{xy} (10^{13} m^5)	λ	*s*	*E* (m)	*S* (m)	θ (°E)
300	5587	130.6	38.3	2.56	1.85	0.02	2550	109	39.5
320	5200	79.1	20.7	2.14	1.96	0.03	2542	141	40.2
340	4649	45.1	10.6	1.85	2.07	0.04	2398	190	41.5
360	4214	23.3	4.79	0.83	2.21	0.04	2261	146	40.5
380	3795	9.34	1.83	0.08	2.26	0.09	2114	32	37.9

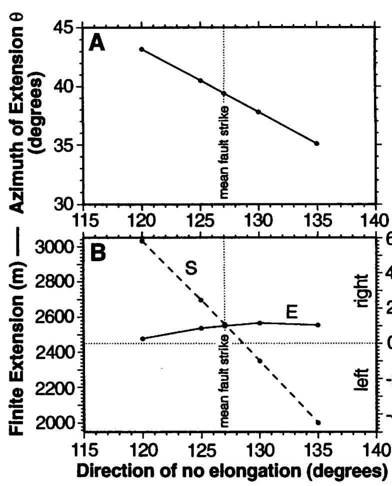

Fig. 8. Sensitivity of determination of azimuth of direction of spreading θ (**A**) and finite extension E and lateral shear S (**B**) on direction of no elongation θ_0.

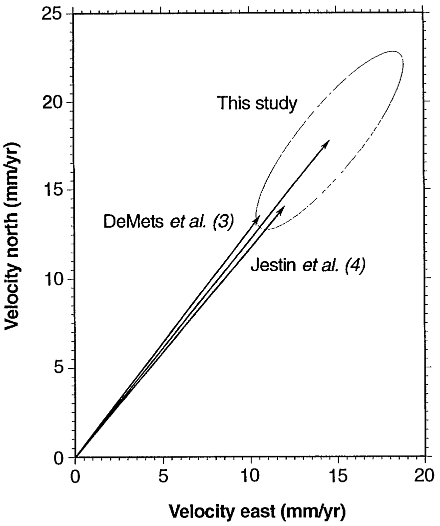

Fig. 9. Spreading vector across the Asal rift. The confidence ellipse was obtained assuming that topography began to record deformation since sometime between 87 and 150 ka and that the azimuth of direction of no elongation lies in the 120 to 135°E range. Arabia-Somalia vectors computed at a point in the Asal rift (11.6°N, 42.5°E) from plate kinematics models (*3, 4*) are shown for comparison.

lows an assessment of the ratio between subsidence and extension over geological time. If we consider dip angles between 60° and 80°, the 700 m of cumulative vertical displacement on the faults accounts for only 5 to 15% of the 2550 m of extension. Injection of dikes and opening of fissures near the surface must have accommodated about 90% of the extension, an amount comparable to that estimated in Iceland (*25*) or along the Mid-Atlantic ridge (*26*). Many such open fissures and dikes have been actually observed in the field (*11*) and show up in the restored topography (Figs. 5A and 7).

Taking the vertical deformation shown in Fig. 5B and the extension by a factor of 1.85 across the rift, we find that the formation of the modern rift has resulted in the subsidence of a volume of $V_1 = 4.3 \times 10^9$ m^3 of crust. From seismic refraction profiles in Afar and near Asal (*27*), it appears that the modern Asal rift has formed in crust that is 5 to 10 km thick. The volume released by 2.6 km of extension along a 10-km-long rift in crust 5 to 10 km thick gives a volume of $V_0 = 125$ to 250×10^9 m^3. Subsidence of the topography therefore accounts for only 1.7 to 3.4% of this volume. The remaining volume must have been filled by magmas from the upper mantle and probably as a result of decompression melting induced by tectonic thinning of the crust. This magma either fed dikes or accumulated at the base of the crust. The lack of a large Bouguer gravity anomaly and the low subsidence at the surface compared to the volume of magmatism suggests that this material has a near crustal density. The recent evolution of the Asal rift has thus been nearly at a steady state, with magmatism compensating for nearly all of the crustal stretching. The subsidence of the topography over the last ~100,000 years and the creation of the Fieale volcano 300 to 100 ka suggests that there have been successive volcanic and tectonic episodes, as has been inferred elsewhere along slow spreading ridges (*13*). However, these episodes reflect only small oscillatory departures of a few percent from the steady state.

A three-dimensional model of deformation across the Asal rift has been derived from the combined analysis of the rift topography and geology. More generally, this approach could allow quantification of deformation and kinematics in areas inaccessible to most direct geophysical and geological investigations, where the main available information is topography or bathymetry. One can conceive of applying this method on mid-oceanic ridges, or possibly to study tectonics and magmatism on other planets.

REFERENCES AND NOTES

1. H. Tazieff, J. Varet, F. Barberi, G. Giglia, *Nature* **235**, 144 (1972).
2. D. P. McKenzie, D. Davies, P. Molnar, *ibid.* **226**, 243 (1970).
3. C. DeMets, R. G. Gordon, D. F. Argus, S. Stein, *Geophys. J. Int.* **101**, 425 (1990).
4. F. Jestin, P. Huchon, J. M. Gaulier, *ibid.* **116**, 637 (1994).
5. P. Tapponnier, R. Armijo, I. Manighetti, V. Courtillot, *Geophys. Res. Lett.* **17**, 1 (1990).
6. G. D. Acton, S. Stein, J. F. Engeln, *Tectonics* **10**, 501 (1991); F. Sigmundsson, *Geophys. Res. Lett.* **19**, 877 (1992); T. Souriot and J.-P. Brun, *Geology* **20**, 911 (1992).
7. V. Courtillot, A. Galdéano, J.-L. Le Mouël, *Earth Planet. Sci. Lett.* **47**, 144 (1980); V. Courtillot *et al., J. Geophys. Res.* **89**, 3315 (1984).
8. A seismic swarm with two earthquakes of magnitude near 5 occurred in the Asal-Ghoubbet rift in November 1978 [A. Abdallah *et al., Nature* **282**, 17 (1979)], showing dominantly left-lateral strike-slip motion [A. Dziewonski, G. Ekström, J. E. Franzen, J. H. Woodhouse, *Phys. Earth Planet. Inter.* **46**, 316 (1987); J.-C. Lépine and A. Hirn, *Tectonophysics* **209**, 65 (1992)]. It was coeval with the 1-week activity of a new eruptive center, the Ardoukoba (Fig. 3) located near the rift axis [P. H. Allard, H. Tazieff, D. Dajlevic, *Nature* **279**, 30 (1979)]. This seismovolcanic event reactivated five to seven inner rift normal faults [A.-Y. Le Dain, B. Robineau, P. Tapponnier, *Bull. Soc. Géol. France* **22**, 817 (1979)] resulting in about 2 m of northeast-southwest extension and 0.7 m of subsidence [J.-C. Ruegg, J.-C. Lépine, A. Tarantola, M. Kasser, *Geophys. Res. Lett.* **6**, 817 (1979)].
9. J.-C. Ruegg, F. Gasse, P. Briole, *C. R. Acad. Sci. Paris* **310**, 1687 (1990).
10. R. S. Stein, P. Briole, J.-C. Ruegg, P. Tapponnier, F. Gasse, *J. Geophys. Res.* **96**, 21789 (1991).
11. A.-Y. Le Dain, B. Robineau, P. Tapponnier, *Bull. Soc. Géol. France* **22**, 817 (1979).
12. J.-B. De Chabalier, H. Sloan, J.-C. Ruegg, Y. Egels, R. S. Stein, *Eos* **72**, 468 (1991).
13. J.-C. Sempéré, J. Lin, H. S. Brown, H. Schouten, G. M. Purdy, *Mar. Geophys. Res.* **15**, 153 (1993).
14. J. Varet, *Geology of Central and Southern Afar (Ethiopia and Djibouti Republic)* (Centre National de la Recherche Scientifique, Paris, 1978), map and 124 pp. report.
15. O. Richard, thesis, Université Paris-Sud, Orsay (1979).
16. L. Stieltjes, *Carte Géologique du Rift d'Asal, Republique de Djibouti (Dépression Afar, Est africain)*, Scale 1:50000 (Centre National de la Recherche Scientifique, Paris, 1980); L. Stieltjes, thesis, Université Paris-Sud, Orsay (1973).
17. K-Ar dates have been made by P.-Y. Gillot and are presented in (*20, 23*).
18. P. Vellutini, *Tectonophysics* **172**, 141 (1990).
19. J. Demange and P. Puvilland, *Le champ géothermique d'Asal, Djibouti, synthèse des données* (Compagnie française pour le développement de la géothermie, report 33CFG06, Orléans, 1993).
20. J.-B. De Chabalier, thesis, Université Paris 7 (1993).
21. F. Gasse and J.-C. Fontes, *Paleogeogr. Paleoclimatol. Paleoecol.* **69**, 67 (1989).
22. L. Zan, G. Gianelli, P. Passerini, C. Troisi, A. O. Haga, *Geothermics* **19**, 561 (1990).
23. I. Manighetti, thesis, Université Paris 6 (1993).
24. D. F. McTigue, *J. Geophys. Res.* **92**, 12931 (1987); L. Chevallier and J. Verwoerd, *ibid.* **93**, 4182 (1988).
25. M. Daignières, V. Courtillot, R. Bayer, P. Tapponnier, *Earth Planet. Sci. Lett.* **26**, 222 (1975).
26. P. A. Cowie, C. H. Scholz, A. Malinverno, M. Edwards, *J. Geophys. Res.* **98**, 17911 (1993).
27. J.-C. Ruegg, *Afar Depression of Ethiopia*, A. Pigler and A. Rösler, Eds. (Schweizerbart, Stuttgart, 1975), vol. 1, pp. 120–134; J. Makris and A. Ginzburg, *Tectonophysics* **141**, 199 (1987).

28. This study was initiated by J.-C. Ruegg and P. Tapponnier. We also benefited from discussions with P.-Y. Gillot, R. Armijo, S. Tait, I. Manighetti, and J. Demange. We thank the French Institut Géographique National for providing the Digital Elevation Model of the Asal rift. We thank G. King and an anonymous reviewer for providing numerous and useful suggestions. This is IPG contribution number 1323.